

## ORIGINAL ARTICLE

# CRIM1 haploinsufficiency causes defects in eye development in human and mouse

Filippo Beleggia<sup>1,2,3</sup>, Yun Li<sup>1,2,3</sup>, Jieqing Fan<sup>4</sup>, Nursel H. Elcioğlu<sup>5</sup>, Ebru Toker<sup>6</sup>, Thomas Wieland<sup>7</sup>, Irene H. Maumenee<sup>8</sup>, Nurten A. Akarsu<sup>9</sup>, Thomas Meitinger<sup>7,10</sup>, Tim M. Strom<sup>7,10</sup>, Richard Lang<sup>4</sup> and Bernd Wollnik<sup>1,2,3,\*</sup>

<sup>1</sup>Institute of Human Genetics, <sup>2</sup>Cologne Excellence Cluster on Cellular Stress Responses in Aging-Associated Diseases (CECAD), <sup>3</sup>Center for Molecular Medicine Cologne (CMMC), University of Cologne, Cologne, Germany, <sup>4</sup>Division of Pediatric Ophthalmology and Division of Developmental Biology, Cincinnati Children's Hospital Medical Center, Cincinnati, OH 45229, USA, <sup>5</sup>Department of Pediatric Genetics, <sup>6</sup>Department of Ophthalmology, Marmara University Medical Faculty, Istanbul, Turkey, <sup>7</sup>Institute of Human Genetics, Helmholtz Zentrum München, Neuherberg, Germany, <sup>8</sup>Illinois Eye and Ear Infirmary, Illinois University, College of Medicine at Chicago, Chicago, IL, USA, <sup>9</sup>Department of Medical Genetics, Gene Mapping Laboratory, Hacettepe University Medical Faculty, Ankara, Turkey and <sup>10</sup>Institute of Human Genetics, Technische Universität München, Munich, Germany

\*To whom correspondence should be addressed at: Institute of Human Genetics, Kerpener Str. 34, Cologne 50931, Germany. Tel: +49 22147886817; Fax: +49 22147886812; Email: bwollnik@uni-koeln.de

## Abstract

Colobomatous macrophthalmia with microcornea syndrome (MACOM, Online Mendelian Inheritance in Man (OMIM) 602499) is an autosomal dominantly inherited malformation of the eye, which is characterized by microcornea with increased axial length, coloboma of the iris and of the optic disc, and severe myopia. We performed whole-exome sequencing (WES) in two affected individuals from the 2p23-p16-linked MACOM family, which includes 13 affected individuals in 3 generations. As no shared novel variation was found on the linked haplotype, we performed copy number variation (CNV) analysis by comparing the coverage of all exons in the WES data sets of the 2 patients with the coverage of 26 control exomes. We identified a heterozygous deletion predicted to span 22 kb including exons 14–17 of CRIM1 (cysteine-rich transmembrane bone morphogenetic protein (BMP) regulator 1). Quantitative PCR (qPCR) analysis confirmed the deletion, which was present in 11 affected individuals. Split-read analysis of WES data followed by breakpoint PCR and Sanger sequencing determined both breakpoints flanked by a 4-bp microhomology (CTTG). In the mouse, *Crim1* is a growth-factor-binding protein with pleiotropic roles in the development of multiple organs, including the eye. To investigate the role of *Crim1* during eye development in mice, we crossed a *Crim1*<sup>fl<sup>ox</sup></sup> mouse line with the *Ap2α-cre* mouse line, which expresses *Cre* in the head surface ectoderm. Strikingly, we observed alterations of eye development in homozygous mice leading to severe anatomical and morphological changes overlapping with the anomalies observed in MACOM patients. Taken together, these findings identify CRIM1 as the causative gene for MACOM syndrome and emphasize the importance of CRIM1 in eye development.

## Introduction

Colobomatous macrophthalmia with microcornea syndrome (MACOM, OMIM 602499) is a rare inherited malformation of the eye which is characterized by microcornea, coloboma of the iris and of the optic disc, increased axial length, staphyloma and severe myopia. Additional associations are increased intraocular pressure, shallow anterior chamber depth and mild cornea plana. The MACOM phenotype has originally been described in an autosomal dominant, 2-generation family with 4 affected individuals (1) and successively in a 4-generation family with 4 affected individuals (2) and in a large 3-generation Turkish family with 13 affected individuals (3). MACOM syndrome seems to be fully penetrant in the reported families, but variable expressivity of the phenotype has been observed, e.g. unilateral presentation (1) and variability in the position and extent of the coloboma, different degrees of corneal diameter reduction and variable severity of macrophthalmia. The severe myopia present in the affected individuals is thought to be secondary to the staphyloma and increased axial length (2).

The vertebrate eye develops from the crosstalk between the optic vesicle, originated from an invagination of the diencephalon, the head surface ectoderm and the ocular mesenchyme near their point of contact. At the time the optic vesicle reaches the head surface ectoderm, their point of contact becomes the lens placode, which then invaginates together with the optic vesicle. The optic vesicle thus becomes the bilayered optic cup, whereas the lens placode develops into the lens vesicle and the head surface ectoderm closing over the lens vesicle becomes the cornea. The ventral margin of the optic cup undergoes an additional invagination. This so-called optic (or choroidal) fissure fuses again later during development generating a canal that provides a route from and into the eye for retinal axons and blood vessels (4). It is thought that the phenotype of MACOM syndrome is probably caused by alterations during this developmental morphogenesis. Microcornea, staphyloma and macrophthalmia are likely to derive from alterations at the level of the head surface ectoderm, which will produce the anterior part of the eye, including cornea and lens, whereas the coloboma derives from the incomplete fusion of the optic fissure (5).

In the large Turkish pedigree initially described by Toker *et al.*, a putative disease locus was mapped to chromosome 2p23-p16, between markers D2S2263 and D2S1352 [positions 28 658 017 and 50 833 825, Genome Reference Consortium Human genome build 37 (GRCh37)] (6). However, the gene is unknown. Here, we report on the identification of cysteine-rich transmembrane BMP regulator 1 (chordin-like) (*CRIM1*) as the causative gene for MACOM syndrome in the family described by Toker *et al.* and, moreover, we demonstrate that a conditional knockout of *Crim1* in mouse craniofacial epidermis causes a very similar developmental eye phenotype.

## Results

### WES in a large Turkish MACOM syndrome pedigree

We obtained DNA samples of 11 affected and 6 healthy individuals from the family described by Toker *et al.* (Fig. 1A). In this large pedigree, the phenotype was characterized by bilateral microcornea (diameter  $\leq 9$  mm), coloboma of the iris, choroid and retina, which involved the optic disc in all but two patients, varying degrees of axial length elongation, myopia, mild cornea plana and shallow anterior chamber (3).

To identify the causative gene in this family, we performed WES on Patients III-1 and III-7 (III-2 and III-9 in Toker *et al.*,

13 and 19 in Elcioglu *et al.*, respectively). For the two exomes, we generated 11.1 and 10.7 gigabases of sequence resulting in an average read depth of 145 and 139, respectively, with 96% of the target regions covered at least 20 times. In total, we obtained 43 306 and 43 211 variations, respectively. After filtering for variants predicted to affect protein sequence or splicing and with a minor allele frequency of  $<0.001$ , only 310 (Patient III-1) and 304 (Patient III-7) variants were left. Of these, three and one variants, respectively, were present in genes located within the linked region described by Elcioglu *et al.* Both patients showed high coverage at these four variant positions, but all four variants were present in only one patient, indicating that these variants are likely located on an unlinked haplotype.

### CNV analysis identifies a large heterozygous deletion in *CRIM1* as the cause of MACOM syndrome

In addition to standard WES analysis, we performed CNV analysis using the program fishingCNV (7), which compares the coverage of all exons in WES data between samples. Using 26 WES data sets from unrelated controls, we identified 110 and 89 statistically significant CNVs ( $P < 0.05$ ), but only one of them was present in both patients and located within the linked interval. This heterozygous, putative deletion was the statistically most significant CNV in both patients ( $P = 1.2 \times 10^{-27}$  and  $P = 6.4 \times 10^{-21}$ ) and predicted to span  $\sim 22$  kb, including exons 14–17 of *CRIM1* (NM\_016441.2) and most of the 3' UTR of *FEZ2* (NM\_001042548.1). To confirm the deletion, we performed qPCR using primers for exon 16 of *CRIM1* in 11 affected individuals and 6 unaffected family members. All of the affected individuals and none of the unaffected family members showed a reduction in the amount of genomic *CRIM1* exon 16 product (Fig. 1B).

To identify the exact breakpoints of the deletion, we analyzed the WES data searching for split-reads that align over the breakpoints. Using the program Pindel (8), we identified the breakpoints at positions 36 757 668 and 36 780 274 of chromosome 2 (GRCh37), flanked by a 4-bp microhomology CTTG sequence. To confirm this result, we performed a breakpoint PCR using primers located in intron 13 of *CRIM1* and intron 8 of *FEZ2*. We were able to amplify a junction fragment in all affected family members, but not in their healthy relatives (Fig. 1C) or in 108 unrelated Turkish controls. We confirmed the location of the breakpoints with Sanger sequencing (Fig. 2A). In addition, we tested DNA from the index patient of the autosomal dominant MACOM family described by Bateman *et al.* (1) for mutations in *CRIM1*. All coding exons of the gene were sequenced, but no causative mutation was found. Moreover, qPCR for the detection of a larger deletion/duplication of *CRIM1* did not detect any alteration indicating further genetic heterogeneity of MACOM syndrome.

*CRIM1* is a transmembrane protein containing six cysteine-rich von Willenbrand factor type C repeat domains (VWFC), an insulin-like growth factor-binding domain, a transmembrane domain and a small cytoplasmic domain (Fig. 1D). It has been reported to function both as a tether for growth factors (9–11) and in the stabilization of adherens junctions through the interaction of its intracellular domain with  $\beta$ -catenin-containing complexes (12).

### The large deletion on chromosome 2 is predicted to affect *CRIM1* but not *FEZ2*

We next identified a C to T polymorphism in exon 6 of *CRIM1* (rs848547) and showed that Patient III-1 is homozygous and Patient III-7 is heterozygous for this single-nucleotide

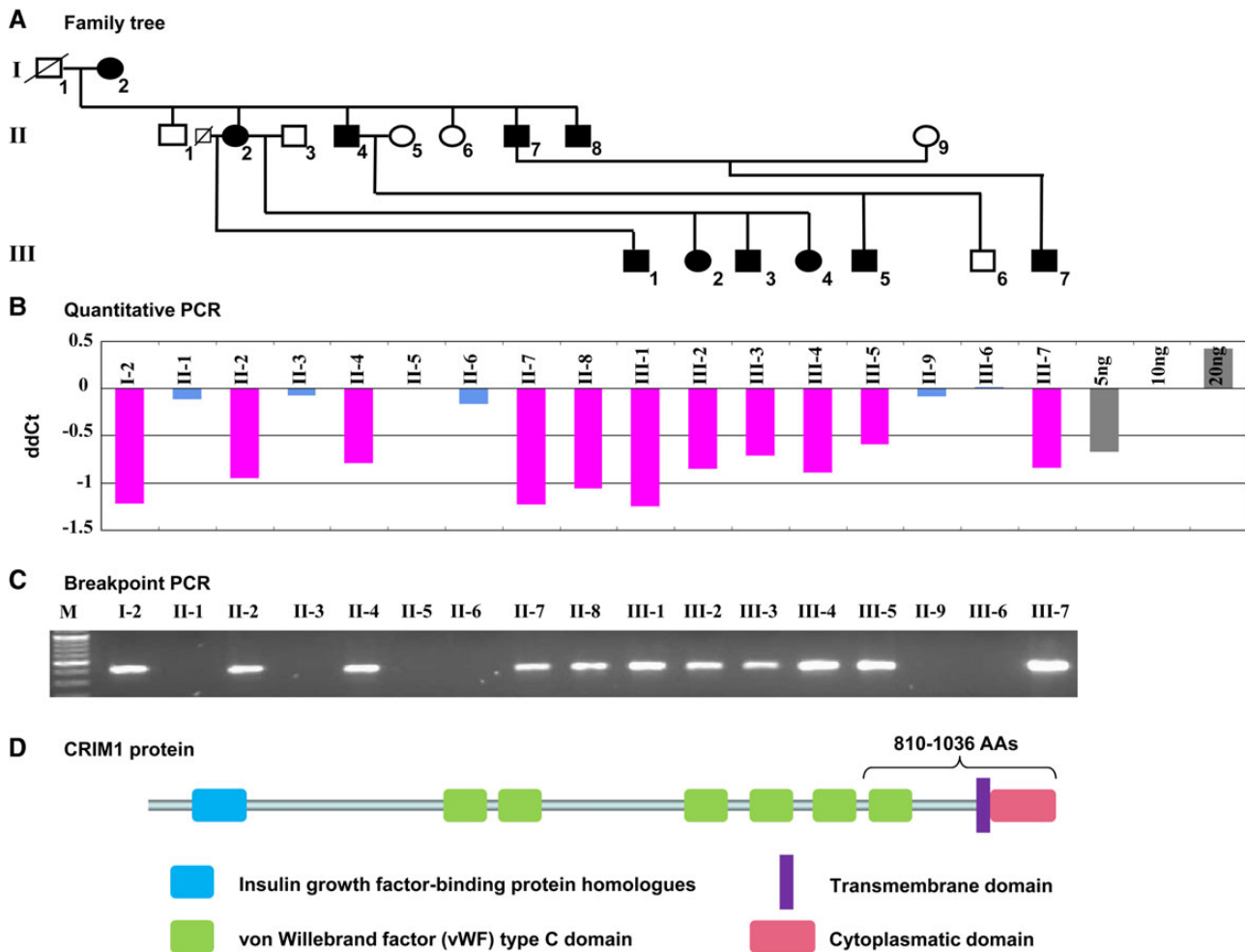


**Figure 1.** Identification of a heterozygous deletion in a large pedigree with MACOM syndrome. (A) Family tree of the pedigree reported by Toker *et al.* including all individuals from whom we obtained DNA samples. (B) Quantitative PCR of exon 6 of *CRIM1*, the delta delta cycle threshold value of 10 ng of control genomic DNA (gDNA) is set to 0. The affected family members show a reduction of *CRIM1* gDNA. (C) Breakpoint PCR: a specific junction fragment could be amplified only in affected family members. (D) Schematic representation of the *CRIM1* protein showing the six VWFC domains, the insulin-like growth factor-binding domain, the transmembrane domain and the cytoplasmic domain. The brackets show the area missing in the deleted allele.

polymorphism (SNP). Using the C/T ratio of rs848547 on complementary DNA (cDNA) derived from blood of Patient III-7, we found that the mutant allele is less abundant and probably undergoes early degradation (Fig. 2B). The deletion spans the last VWFC domain, the transmembrane domain and the cytoplasmic domain and is therefore predicted to prevent both the tethering function of *CRIM1* and its interaction with  $\beta$ -catenin-containing complexes. In addition, we tested whether the partial deletion of the FEZ2 3' UTR might have an influence on RNA levels and thereby contribute to the phenotype. Again, we used a heterozygous A to G polymorphism in exon 3 of FEZ2 (rs14291) found in Patient III-7. Sanger sequencing of patients' cDNA did not reveal any significant reduction in the amount of the mutant allele (Fig. 2B).

#### Loss of *Crim1* in the developing eye of the mouse causes a phenotype similar to human MACOM syndrome

A loxP *Crim1* conditional mouse line (*Crim1*<sup>fl<sup>ox</sup></sup>) has recently been generated (9). When crossed with a germline expressing cre line, the mice showed perinatal lethality, multiple developmental abnormalities and an eye phenotype characterized by small lenses,

restricted aperture of the anterior eye chamber and accumulation of cells in the posterior eye chamber (9). To further characterize the effects of *Crim1* loss of function during eye development, we crossed the loxP *Crim1* conditional mouse line with an *Ap2 $\alpha$ -cre* line (13). *Ap2 $\alpha$ -cre* is expressed in the head surface ectoderm and ocular mesenchyme of the mouse embryo (14), i.e. exactly the tissues from which the cornea and lens develop. Heterozygous mice were healthy and showed no particular phenotype. Strikingly, the eyes of the homozygous *Crim1*<sup>fl<sup>ox</sup>/fl<sup>ox</sup></sup>*Ap2 $\alpha$ -cre* mice showed morphological changes overlapping with the developmental eye anomalies present in patients with MACOM syndrome, including microcornea, a shallow anterior chamber and a narrower eye without diminished axial diameter (Fig. 3A and B). Additionally, the lens of the *Crim1*<sup>fl<sup>ox</sup>/fl<sup>ox</sup></sup>*Ap2 $\alpha$ -cre* mice is smaller and pear-shaped and often shows deficient development of the fiber cell mass (Fig. 3C and D), which might indicate a defect in cell adhesion.

#### Discussion

In this study, we identify *CRIM1* as the causative gene for MACOM syndrome, and we show that loss of *Crim1* in the mouse tissues

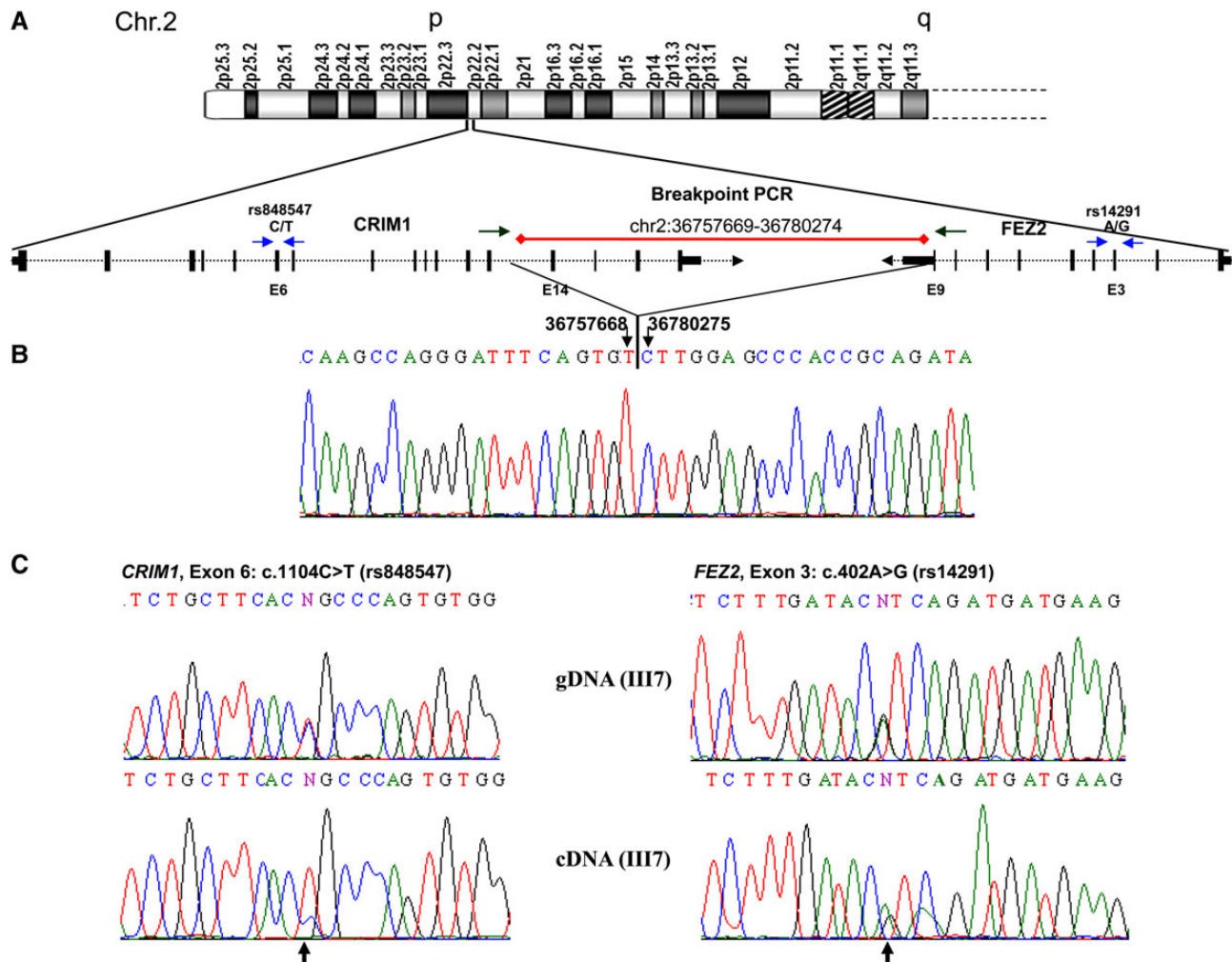


**Figure 2.** A ~22-kb deletion of CRIM1 causes MACOM syndrome. (A) Panel A shows the position of CRIM1 within chromosome 2 and its genomic organization. The red bar shows the deletion, including the last four exons of CRIM1 and most of the 3' UTR of FEZ2. The green arrows show the positions of the breakpoint PCR primers; the blue arrows show the positions of the primers used for quantifying the transcripts of CRIM1 and FEZ2. (B) Chromatogram showing the breakpoints at positions 36 757 668 and 36 780 275. (C) Comparison of chromatograms from gDNA and cDNA to quantify the relative amounts of deleted and non-deleted alleles of CRIM1 (left) and FEZ2 (right). For CRIM1, rs848547 (black arrow) shows a cytosine on the deleted allele, which is strongly reduced in the cDNA chromatogram. For FEZ2, rs14291 shows a guanosine in the deleted allele, which is slightly reduced at cDNA level.

responsible for eye development causes a phenotype that is very similar to human MACOM syndrome.

We performed WES on two affected individuals from the large MACOM pedigree first published by Toker *et al.* (3). In the same family, Elcioglu *et al.* performed linkage analysis and identified the maximum possible LOD score of 3.61 in a candidate region on chromosome 2. Consistent with the large number of family members included in the linkage analysis, the probability of producing an LOD score of 3.61 by chance is very low ( $P \leq 0.0001$ ) (6). We therefore focused the search for the causative gene on this region, but we could not identify any candidate mutation after the initial analysis. However, using only data derived from WES, we successfully identified the large heterozygous deletion in CRIM1 by comparing the coverage of the patient samples over all exons to the coverage of unrelated controls.

Additionally, we directly identified the exact breakpoints of the deletion from the WES data using a split-read approach. The split-read approach is unlikely to succeed in WES experiments, because the enriched region represents <2% of the genome, so that breakpoints can only be identified if they are located within or very close

to the target region. In our case, both breakpoints were outside of the target region, but the 36 780 274 breakpoint was close enough to the last exon of FEZ2 to be covered by four reads in Patient III-1 and five reads in Patient III-7.

While the precise mutational mechanism is unknown, the absence of long homologous stretches or repetitive elements near the breakpoints argues against non-allelic homologous recombination (15). Furthermore, the presence of a 4-bp microhomology (CTTG) suggests that the deletion was caused either by error-prone DNA repair mechanisms, such as non-homologous end joining (16), or by DNA replication-based mechanisms, such as microhomology-mediated break-induced replication (17) or fork stalling and template switching (FoSTeS) (18).

Two different heterozygous deletions reported in the Decipher database include CRIM1, but the large number of additional genes involved in these deletions (30 and 28, respectively) and the incomplete descriptions of the phenotypes prevent a direct comparison with the family studied in this paper. The Exome Variant Server reports a frameshift variant in 3 out of 12 516 alleles and a nonsense mutation in 1 out of 13 005 alleles. The frameshift



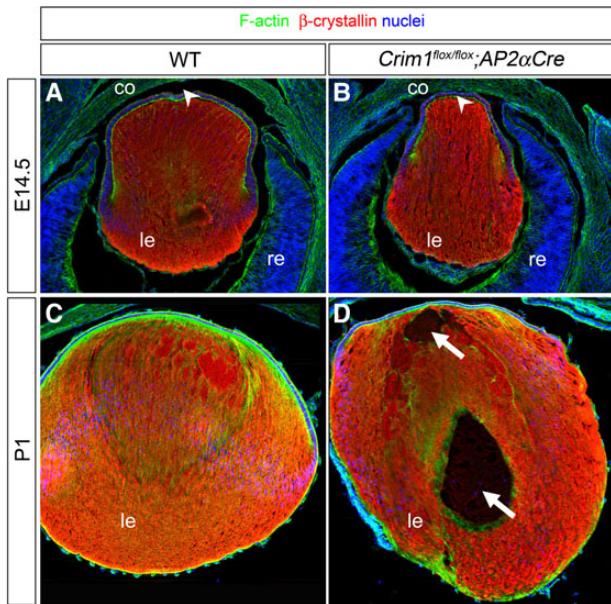


**Figure 3.** *Crim1*<sup>flox/flox</sup>Ap2 $\alpha$ -cre showed morphological changes overlapping with the developmental eye anomalies present in patients with MACOM syndrome.  $\beta$ -crystalline labeling showing the eye phenotype of *Crim1*<sup>flox/flox</sup>; Ap2 $\alpha$ -cre (B, D) compared with WT (A, C) mice. (A, B) At embryonic day 14.5, anomalies are obvious in the eyes of *Crim1*<sup>flox/flox</sup>Ap2 $\alpha$ -cre mice. There is a shallower anterior chamber (arrowheads), microcornea with normal axial length and a narrower pear-shaped lens. (C, D) Close-up view of the lens at postnatal day 1, showing multiple anomalies in the fiber cell mass of *Crim1*<sup>flox/flox</sup>Ap2 $\alpha$ -cre mice (arrows). Representative figures of the 12 mice analyzed at E14.5 and the 7 mice analyzed at P1 are shown. co, cornea; le, lens; re, retina.

variant is predicted to only affect the last four amino acids of CRIM1 and is thus unlikely to be a true loss-of-function allele. The nonsense mutation could represent a sequencing artifact, or if present, a truncated protein might have a different functional effect not leading to developmental eye anomalies. We did not detect any causative mutation in the index patient of the autosomal dominant MACOM family described by Bateman *et al.* (1) indicating further genetic heterogeneity of MACOM syndrome.

CRIM1 was first identified as an interactor of Wilms tumor 1 (19) and is expressed in numerous mouse tissues including developing eye, kidney, blood vessels, brain and limb (20–23). The homozygous *Crim1* hypomorph KST264 mouse as well as two described conditional *Crim1* knockdown mice showed perinatal lethality and multiple developmental abnormalities of the eye, kidney, limbs and placenta. The eye phenotype in these mice is characterized by small lenses, restricted aperture of the anterior eye chamber and accumulation of cells in the posterior eye chamber (9,10,23–25). *Crim1* is thought to have both an extracellular function as a tether, which binds growth factors such as BMPs, vascular endothelial growth factor A and platelet-derived growth factor, modulating their activity (9–11), and an intracellular function, where the *Crim1* cytoplasmic domain binds in a complex with  $\beta$ -catenin and cadherins, important for cell–cell adhesion (12). In the developing eye, *Crim1* expression is detected in the optic vesicle, optic cup, ocular mesenchyme and head surface ectoderm, and expression is especially high in the lens, the only ocular tissue where it persists after development (22).

Given the perinatal lethality and wide range of affected tissues in the ubiquitous *Crim1* hypomorph and knockdown mice, we crossed the conditional loxP *Crim1* mouse line with an Ap2 $\alpha$ -cre line, which expresses cre in the head surface ectoderm

and ocular mesenchyme. The resulting *Crim1*<sup>flox/flox</sup>Ap2 $\alpha$ -cre mice show a phenotype remarkably similar to human MACOM syndrome, including microcornea, shallow anterior chamber and a narrow eye without diminished axial diameter. We have not found any colobomas in the *Crim1*<sup>flox/flox</sup>Ap2 $\alpha$ -cre mice, probably because Ap2 $\alpha$  is not expressed in tissues responsible for coloboma formation.

As *Crim1* has different functions, it is an interesting working hypothesis for future experiments to determine whether the extracellular or the intracellular CRIM1 function is mainly responsible for the observed eye phenotype. As an extracellular tether, *Crim1* could modulate the action of different growth factors such as the BMPs and transforming growth factor- $\beta$  2, which have been shown to play an important role during eye development and in the fusion of the optic fissure (26–29). *Crim1* haploinsufficiency could thus alter growth factor expression and function. Alternatively, haploinsufficiency could act on the intracellular function of *Crim1* as an interactor of  $\beta$ -catenin and cadherins, causing a destabilization of adherens junctions during eye development and closure of the optic fissure (30–32).

Taken together, our data identify CRIM1 as the causative gene for MACOM syndrome and emphasize the importance of CRIM1 in eye development in both human and mouse.

## Materials and Methods

### Human subjects

All subjects or their legal representatives gave written informed consent to the study. The study was performed in accordance with the Declaration of Helsinki protocols and approved by the local institutional review boards. DNA from participating family members was extracted from peripheral blood lymphocytes by standard extraction procedures.

### Whole-exome sequencing

Exonic and adjacent intronic regions were enriched from genomic DNA using the 50-Mb SureSelect Human All Exon enrichment kit, and sequencing was performed with a GAIIX sequencer from Illumina. Alignment against the GRCh37 human reference was performed with Burrows-Wheeler Aligner (BWA) (33), PCR-duplicates marking with Picard, indel realignment, base quality recalibration and variant calling with genome analysis toolkit (GATK) (34) and annotation with Annovar (35). The resulting variants were filtered to exclude variants present in dbSNP, the Exome Variant Server, the 1000 Genomes Project, and our in-house database and variants that were not predicted to affect protein sequence or exon splicing. CNV analysis was performed using the program fishingCNV (7) with 26 unrelated controls. Breakpoint analysis was performed using the program Pindel (8).

### Breakpoint PCR and qPCR analysis

Breakpoint PCR was performed using primers designed to anneal outside of the deleted region, with the forward primer located in intron 13 of CRIM1 and the reverse primer located in intron 8 of FEZ2. The resulting products were sequenced using the chain termination method (36). qPCR was performed using the taqman assay from Integrated DNA Technologies, and the results were analyzed using the  $\Delta\Delta$ Ct-method as previously described (37).

### Comparison of allele quantity at cDNA and genomic DNA level

RNA was extracted from fresh blood using the Paxgene blood RNA system from Qiagen. RT-PCR was performed using the RevertAid

First Strand cDNA Synthesis Kit from Thermo Scientific. The regions containing the SNP rs848547 for CRIM1 and the SNP rs14291 for FEZ2 were amplified from both genomic DNA and cDNA and sequenced with the chain termination method (36).

### Generation of the Crim1<sup>flox/flox</sup>Ap2 $\alpha$ -cre mouse model

Animals were housed in accordance with institutional policies. Crim1<sup>flox</sup> and AP2 $\alpha$ -cre mice have been described previously (9,14). Gestational age was determined through detection of a vaginal plug. Tissues were fixed in 4% paraformaldehyde and cryopreserved in optimal cutting temperature (OCT). Twelve-micrometer cryosections were cut, and immunofluorescence labeling of cryosections was performed as described (38), with beta-crystalline antibody (1:5000, homemade) and Alexa 594 anti-rabbit secondary antibody. Phalloidin-Alexa 488 and Hoechst 33258 were used to label filamentous actin and nuclei, respectively.

### Web Resources

UCSC browser: <http://genome.ucsc.edu/index.html>  
 PolyPhen: <http://genetics.bwh.harvard.edu/pph2/>  
 UniProt: <http://www.uniprot.org/>  
 OMIM: <http://www.omim.org/>  
 The Exome Variant Server: <http://evs.gs.washington.edu/EVS/>  
 NCBI: <http://www.ncbi.nlm.nih.gov/>  
 Ensembl: <http://www.ensembl.org/index.html>  
 BWA: <http://bio-bwa.sourceforge.net/>  
 GATK: <https://www.broadinstitute.org/gatk/>  
 Annovar: <http://www.openbioinformatics.org/annovar/>  
 Picard: <http://broadinstitute.github.io/picard>  
 Decipher database: <http://decipher.sanger.ac.uk>

### Acknowledgements

We are grateful to all family members who participated in this study and to Karin Boss for critically reading the manuscript.

Conflict of Interest statement. None declared.

### Funding

This work was supported by German Federal Ministry of Education and Research grants O1GM1211A (E-RARE network CRANIR-ARE-2) and O1GM1109C (FACE, national rare disease network 'Forschungsverbund Ausgewählter Craniofacialer Entwicklungsstörungen') to B.W. This study makes use of data generated by the DECIPHER Consortium. A full list of centres who contributed to the generation of the data is available from <http://decipher.sanger.ac.uk> and via email from [decipher@sanger.ac.uk](mailto:decipher@sanger.ac.uk). Funding for the project was provided by the Wellcome Trust.

### References

- Bateman, J.B. and Maumenee, I.H. (1984) Colobomatous macrophthalmia with microcornea. *Ophthalmic Paediatr. Genet.*, **4**, 59–66.
- Pallotta, R., Fusilli, P., Sabatino, G., Verrotti, A. and Chiarelli, F. (1998) Confirmation of the colobomatous macrophthalmia with microcornea syndrome: report of another family. *Am. J. Med. Genet.*, **76**, 252–254.
- Toker, E., Elcioglu, N., Ozcan, E., Yenice, O. and Ogut, M. (2003) Colobomatous macrophthalmia with microcornea syndrome: report of a new pedigree. *Am. J. Med. Genet. A*, **121A**, 25–30.
- Chow, R.L. and Lang, R.A. (2001) Early eye development in vertebrates. *Annu. Rev. Cell. Dev. Biol.*, **17**, 255–296.
- Chang, L., Blain, D., Bertuzzi, S. and Brooks, B.P. (2006) Uveal coloboma: clinical and basic science update. *Curr. Opin. Ophthalmol.*, **17**, 447–470.
- Elcioglu, N.H., Akin, B., Toker, E., Elcioglu, M., Kaya, A., Tuncali, T., Wollnik, B., Hornby, S. and Akarsu, N.A. (2007) Colobomatous macrophthalmia with microcornea syndrome maps to the 2p23-p16 region. *Am. J. Med. Genet. A*, **143A**, 1308–1312.
- Shi, Y. and Majewski, J. (2013) FishingCNV: a graphical software package for detecting rare copy number variations in exome-sequencing data. *Bioinformatics*, **29**, 1461–1462.
- Ye, K., Schulz, M.H., Long, Q., Apweiler, R. and Ning, Z. (2009) Pindel: a pattern growth approach to detect break points of large deletions and medium sized insertions from paired-end short reads. *Bioinformatics*, **25**, 2865–2871.
- Fan, J., Ponferrada, V.G., Sato, T., Vemaraju, S., Fruttiger, M., Gerhardt, H., Ferrara, N. and Lang, R.A. (2014) Crim1 maintains retinal vascular stability during development by regulating endothelial cell Vegfa autocrine signaling. *Development*, **141**, 448–459.
- Wilkinson, L., Gilbert, T., Kinna, G., Ruta, L.A., Pennisi, D., Kett, M. and Little, M.H. (2007) Crim1KST264/KST264 mice implicate Crim1 in the regulation of vascular endothelial growth factor-A activity during glomerular vascular development. *J. Am. Soc. Nephrol.*, **18**, 1697–1708.
- Wilkinson, L., Kolle, G., Wen, D., Piper, M., Scott, J. and Little, M. (2003) CRIM1 regulates the rate of processing and delivery of bone morphogenetic proteins to the cell surface. *J. Biol. Chem.*, **278**, 34181–34188.
- Ponferrada, V.G., Fan, J., Vallance, J.E., Hu, S., Mamedova, A., Rankin, S.A., Kofron, M., Zorn, A.M., Hegde, R.S. and Lang, R.A. (2014) CRIM1 complexes with  $\beta$ -catenin and cadherins, stabilizes cell-cell junctions and is critical for neural morphogenesis. *PLoS One*, **7**, e32635.
- Macatee, T.L., Hammond, B.P., Arenkiel, B.R., Francis, L., Frank, D.U. and Moon, A.M. (2003) Ablation of specific expression domains reveals discrete functions of ectoderm- and endoderm-derived FGF8 during cardiovascular and pharyngeal development. *Development*, **130**, 6361–6374.
- Song, N., Schwab, K.R., Patterson, L.T., Yamaguchi, T., Lin, X., Potter, S.S. and Lang, R.A. (2007) pygopus 2 has a crucial, Wnt pathway-independent function in lens induction. *Development*, **134**, 1873–1885.
- Hastings, P.J., Lupski, J.R., Rosenberg, S.M. and Ira, G. (2009) Mechanisms of change in gene copy number. *Nat. Rev. Genet.*, **10**, 551–564.
- Lieber, M.R. (2008) The mechanism of human nonhomologous DNA end joining. *J. Biol. Chem.*, **283**, 1–5.
- Hastings, P.J., Ira, G. and Lupski, J.R. (2009) A microhomology-mediated break-induced replication model for the origin of human copy number variation. *PLoS Genet.*, **5**, e1000327.
- Lee, J.A., Carvalho, C.M. and Lupski, J.R. (2007) A DNA replication mechanism for generating nonrecurrent rearrangements associated with genomic disorders. *Cell*, **131**, 1235–1247.
- Kolle, G., Georgas, K., Holmes, G.P., Little, M.H. and Yamada, T. (2000) CRIM1, a novel gene encoding a cysteine-rich repeat protein, is developmentally regulated and implicated in

- vertebrate CNS development and organogenesis. *Mech. Dev.*, **90**, 181–193.
20. Georgas, K., Bowles, J., Yamada, T., Koopman, P. and Little, M.H. (2000) Characterisation of *Crim1* expression in the developing mouse urogenital tract reveals a sexually dimorphic gonadal expression pattern. *Dev. Dyn.*, **219**, 582–587.
  21. Glienke, J., Sturz, A., Menrad, A. and Thierauch, K.H. (2002) *CRIM1* is involved in endothelial cell capillary formation in vitro and is expressed in blood vessels in vivo. *Mech. Dev.*, **119**, 165–175.
  22. Lovicu, F.J., Kolle, G., Yamada, T., Little, M.H. and McAvoy, J.W. (2000) Expression of *Crim1* during murine ocular development. *Mech. Dev.*, **94**, 261–265.
  23. Pennisi, D.J., Wilkinson, L., Kolle, G., Sohaskey, M.L., Gillinder, K., Piper, M.J., McAvoy, J.W., Lovicu, F.J. and Little, M.H. (2007) *Crim1KST264/KST264* mice display a disruption of the *Crim1* gene resulting in perinatal lethality with defects in multiple organ systems. *Dev. Dyn.*, **236**, 502–511.
  24. Chiu, H.S., York, J.P., Wilkinson, L., Zhang, P., Little, M.H. and Pennisi, D.J. (2012) Production of a mouse line with a conditional *Crim1* mutant allele. *Genesis*, **50**, 711–716.
  25. Pennisi, D.J., Kinna, G., Chiu, H.S., Simmons, D.G., Wilkinson, L. and Little, M.H. (2012) *Crim1* has an essential role in glycogen trophoblast cell and sinusoidal-trophoblast giant cell development in the placenta. *Placenta*, **33**, 175–182.
  26. Adler, R. and Belecky-Adams, T.L. (2002) The role of bone morphogenetic proteins in the differentiation of the ventral optic cup. *Development*, **129**, 3161–3171.
  27. Morcillo, J., Martinez-Morales, J.R., Trousse, F., Fermin, Y., Sowden, J.C. and Bovolenta, P. (2006) Proper patterning of the optic fissure requires the sequential activity of *BMP7* and *SHH*. *Development*, **133**, 3179–3190.
  28. Saika, S., Saika, S., Liu, C.Y., Azhar, M., Sanford, L.P., Doetschman, T., Gendron, R.L., Kao, C.W. and Kao, W.W. (2001) *TGFbeta2* in corneal morphogenesis during mouse embryonic development. *Dev. Biol.*, **240**, 419–432.
  29. Weston, C.R., Wong, A., Hall, J.P., Goad, M.E., Flavell, R.A. and Davis, R.J. (2003) *JNK* initiates a cytokine cascade that causes *Pax2* expression and closure of the optic fissure. *Genes. Dev.*, **17**, 1271–1280.
  30. Chen, S., Lewis, B., Moran, A. and Xie, T. (2012) Cadherin-mediated cell adhesion is critical for the closing of the mouse optic fissure. *PLoS One*, **7**, e51705.
  31. Masai, I., Lele, Z., Yamaguchi, M., Komori, A., Nakata, A., Nishiwaki, Y., Wada, H., Tanaka, H., Nojima, Y., Hammerschmidt, M. et al. (2003) *N-cadherin* mediates retinal lamination, maintenance of forebrain compartments and patterning of retinal neurites. *Development*, **130**, 2479–2494.
  32. Westenskow, P., Piccolo, S. and Fuhrmann, S. (2009) *Beta-catenin* controls differentiation of the retinal pigment epithelium in the mouse optic cup by regulating *Mitf* and *Otx2* expression. *Development*, **136**, 2505–2510.
  33. Li, H. and Durbin, R. (2009) Fast and accurate short read alignment with Burrows-Wheeler transform. *Bioinformatics*, **25**, 1754–1760.
  34. DePristo, M.A., Banks, E., Poplin, R., Garimella, K.V., Maguire, J. R., Hartl, C., Philippakis, A.A., del Angel, G., Rivas, M.A., Hanna, M. et al. (2011) A framework for variation discovery and genotyping using next-generation DNA sequencing data. *Nat. Genet.*, **43**, 491–498.
  35. Wang, K., Li, M. and Hakonarson, H. (2010) ANNOVAR: functional annotation of genetic variants from high-throughput sequencing data. *Nucl. Acids Res.*, **38**, e164.
  36. Sanger, F., Nicklen, S. and Coulson, A.R. (1977) DNA sequencing with chain-terminating inhibitors. *Proc. Natl Acad. Sci. USA*, **74**, 5463–5467.
  37. Li, Y., Pabst, S., Lokhande, S., Grohe, C. and Wollnik, B. (2009) Extended genetic analysis of *BTNL2* in sarcoidosis. *Tissue Antigens*, **73**, 59–61.
  38. Smith, A.N., Miller, L.A., Song, N., Taketo, M.M. and Lang, R.A. (2005) The duality of *beta-catenin* function: a requirement in lens morphogenesis and signaling suppression of lens fate in periocular ectoderm. *Dev. Biol.*, **285**, 477–489.